The Hierarchical Structure of Water-Assisted Injection Molded High Density Polyethylene: Small Angle X-ray Scattering Study

Xianhu Liu,[1] Guoqiang Zheng,[1,2] Zhenhua Jia,[1] Songwei Li,[1] Chenggang Liu,[1] Yang Zhang,[1] Chunguang Shao,[1] Kun Dai,[1] Baochen Liu,[1] Qinxing Zhang,[1] Songjie Wang,[1] Chuntai Liu,[1] Jingbo Chen,[1] Xiangfang Peng,[2] Changyu Shen[1]

[1]*College of Materials Science and Engineering, The Key Laboratory of Advanced Materials Processing and Mold of Ministry of Education, Zhengzhou University, Zhengzhou, Henan 450002, People's Republic of China*
[2]*The Key Laboratory of Polymer Processing Engineering, Ministry of Education, Guangzhou, Guangdong 510641, People's Republic of China*

Received 12 December 2010; accepted 22 March 2011
DOI 10.1002/app.36408
Published online 22 Janaury 2012 in Wiley Online Library (wileyonlinelibrary.com).

ABSTRACT: High density polyethylene (HDPE) was molded by a new polymer processing method, that is, water-assisted injection molding (WAIM), and its hierarchical structure was studied by two-dimensional small angle X-ray scattering (SAXS). For comparison, the hierarchical structure of HDPE molded by conventional injection molding (CIM) was also characterized. The result shows that the WAIM part exhibits a distinct skin-core-water channel structure which is different from the skin-core structure for the CIM part. In the skin layer of both WAIM and CIM parts, the shish-kebab structure was formed due to the shear stress brought by melt filling, but the lamellar orientation parameter of CIM part is smaller than that of WAIM part. The spherulites with random lamellar orientation are dominant at the core of both parts owing to the low cooling rate and feeble shear stress therein. Interestingly, the shish structure and the lamellae with low level of orientation can be found at the water channel layer of WAIM part. They are attributed to the shear stress brought by water penetration. Moreover, the lamellar orientation parameter in water channel layer is smaller than that of skin layer. In addition, the long period of WAIM part first increases and then decreases with the elevating distance from the skin surface, while that of CIM part tends to increase monotonously. In a word, one can conclude that the rapid cooling rate and shear brought by the injected water have significant influence on the structural evolution for the WAIM part. J Appl Polym Sci 125: 2297–2303, 2012

Key words: water-assisted injection molding; lamellar; orientation; polyethylene (PE); SAXS

INTRODUCTION

Water-assisted injection molding (WAIM) is an innovative polymer processing method for the preparation of hollow parts. Generally, according to the volume of injected melt, WAIM can be divided into short-shot process and full-shot process. As for the short-shot process, a schematic diagram of its procedure is illustrated in Figure 1(a). Clearly, it can be divided into three stages: first, the cavity is partially filled with polymer melt; second, the high-pressure water is injected into the core of the polymer melt; third, the water continues to pack the melt till the melt is solidified. Compared with conventional injection molding (CIM), WAIM has many advantages,[1–7] such as the light weight of WAIM products, relatively lower resin cost per part, shorter cycle time as well as its flexibility in the design and manufacture of plastic parts. In addition, some defects encountered in CIM, such as residual stress, warpage, and shrinkage, can be substantially eliminated, especially for the large parts whose quality and rigidity are the main concerns when using WAIM. Therefore, WAIM has received great attention recently.

In the CIM process, it is well known that polymer melt is subjected to an intricate thermo-mechanical field characterized by fast cooling rate, severe stress field, and such thermo-mechanical history in return does play an important role in the development of morphological features.[3–12] It also has well established that shear flow can not only accelerate the crystallization process of semicrystalline polymers but also induce some interesting crystalline morphology such as shish-kebab.[12–14] Moreover, according to the morphological features, numerous researchers[8–10] have demonstrated that polymers molded by CIM are always characterized with typical skin-core structure.

Correspondence to: Zheng (gqzheng@zzu.edu.cn) or C. Shen (shency@zzu.edu.cn).

Contract grant sponsor: National Nature Science Foundation of China; contract grant numbers: 50803060, 10872186 and 10872185.

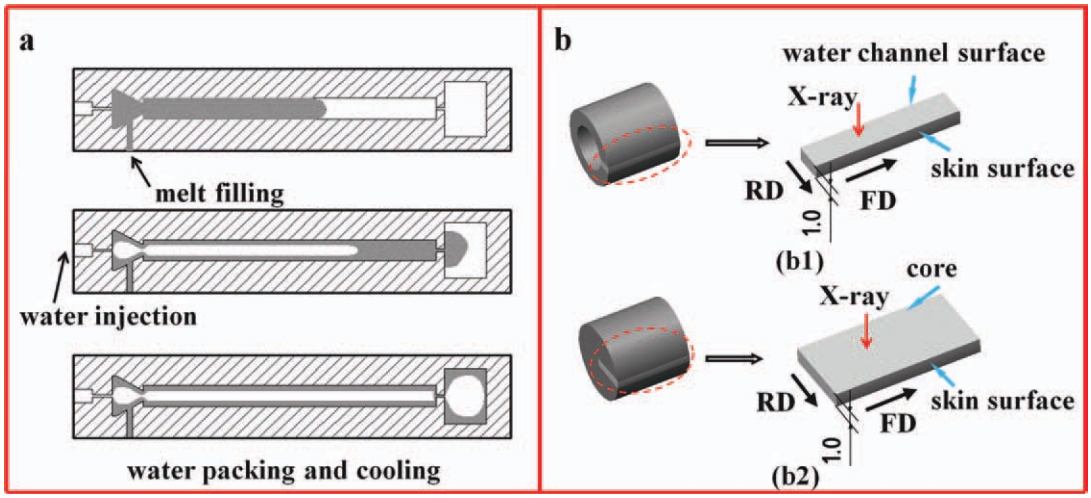

Figure 1 (a) Schematic diagram of full-shot with an overfill cavity of WAIM process; (b) Detected positions for 2D SAXS measurement of (b1) WAIM part and (b2) CIM part. [Color figure can be viewed in the online issue, which is available at wileyonlinelibrary.com.]

As clearly shown in Figure 1(a), polymer melt in the WAIM process is confined not only by the mold wall but also by the injected water. Furthermore, during the WAIM process, melt is compelled to successively flow twice (i.e., the flow respectively brought by the melt filling and the injected water). More importantly, the injected water has a significant effect of rapid cooling rate on the interior melt. Obviously, it is unambiguous that the thermo-mechanical field in WAIM process is more complicated than that in CIM process. As a result, it can be envisaged that a more interesting morphology will be formed during WAIM process.

So far, there are a few studies available on the evolution of phase morphology in the WAIM parts. Liu et al.[3,4] investigated the fiber orientation and crystallinity in the glass fiber reinforced polypropylene and poly-butylene-terephthalate composites. It was found that fiber highly oriented in the mold/polymer interface and the crystallinity increases with the increasing injected water temperature. The morphological development in fluids (water and gas) assisted injection molded high density polyethylene (HDPE)/PC and HDPE/PA-6 blends were also comparatively studied,[5,6] and the scanning electron microscope results showed that the shape and size of the dispersed phase depend on the position along both the part thickness and the flow direction (FD). Recently, Huang and Zhou[8] have reported the development of phase morphology in blend molded by WAIM, and the results showed that the phase morphology varies significantly across the thickness of the residual wall. It concluded that the water penetration has a substantial influence on the deformation of dispersed phase. According to the different morphology features described in the literatures,[6,8] a distinct skin-core-water channel structure across the thickness were defined in the WAIM part.

To the best of the authors' knowledge, studies on the crystalline morphology of the semicrystalline polymer molded by WAIM are scarcely found in the open literatures. In this article, our interest lies in the hierarchical structure, especially the distribution of oriented structure, of HDPE molded by WAIM. For comparison, the hierarchical structure of CIM part was also investigated. It was found that shear brought by injected water can induce the development of shish structure in the water channel layer. Furthermore, the injected water exhibits significant role in preserving the orientation in the water channel layer as well as that in the skin layer induced by melt filling. The results obtained are helpful to further understand the relationship between the physical fields during WAIM process and the evolution of the crystalline orientation.

EXPERIMENTAL

Material

A commercial grade HDPE (5000S, Daqing Petroleum Chemical Co., China), with a number average molecular weight of 5.28×10^5 g/mol and a melt flow rate of 0.9 g/10 min (190°C, 21.6 N), was used in the form of pellets.

Specimen preparation

WAIM and CIM parts' profile is of cylindrical shape, with a diameter of 10 mm and a length of 300 mm. The main body of CIM part exhibits a solid structure, while that of WAIM part is of a hollow one.

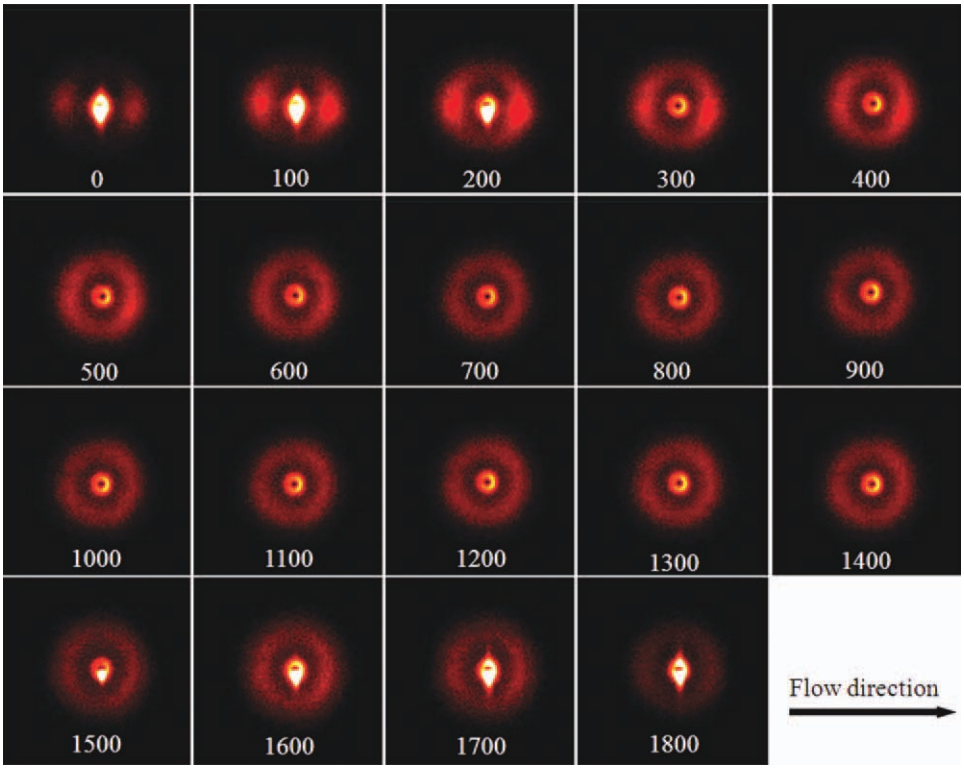

Figure 2 2D SAXS image patterns at different distances from the skin surface to water channel surface of WAIM part. The number (in μm) on each image represents the distance away from skin surface. [Color figure can be viewed in the online issue, which is available at wileyonlinelibrary.com.]

A controllable high-pressure water injection equipment, which mainly consists of a high-pressure water generator and conveying unit, water injector and water injection pin with an inner orifice, was recently developed in our laboratory. A HTF80B-W2 CIM machine was used to inject melt. The barrel temperature from the hopper to nozzle of the machine was 170, 190, 220, and 205°C. The melt and water injection pressure was 75 and 15 MPa, respectively. The water injection delay time was 1 s. The processing parameters used for the CIM parts were identical with those for the WAIM parts, except that the former was free from water injection and packing. Both mold and water were kept at room temperature in the molding.

Two-dimensional small angle X-ray scattering measurements

The two-dimensional (2D) small angle X-ray scattering (SAXS) measurements were performed using a NanoSTAR-U (Bruker AXS INC.) with Cu Kα radiation source ($\lambda = 0.154$ nm) at room temperature. Before 2D SAXS measurement, a segment with 10 mm length (i.e., the FD) of the WAIM and CIM parts is cut in the middle of the part, from which a board of 1 mm thickness was grinded along FD-residual wall direction (RD) plane. The selected positions for 2D SAXS measurements were taken from the surface along the RD, which is schematically illustrated in Figure 1(b). The X-ray beam is then perpendicular to FD-RD plane. The generator was operated at 45 kV and 650 μA. The 2D SAXS intensity was collected with a 2D gas-filled wire detector (Bruker Hi-Star). The distance from the sample to detector was 1070.5 mm. Typical collection time is 10 min. Because of the geometrical symmetry for both WAIM and CIM parts, only one half-width of a specimen was illuminated in the experiments.

RESULTS

The distribution of lamellar orientation for the WAIM part

Figure 2 shows the 2D SAXS patterns at different positions from the skin surface to water channel surface of the WAIM part. It is clear that a two-crescent equatorial maximum and a distinct meridional streak are observed at 0, 100, and 200 μm. The simultaneous occurrence of meridional and equatorial maxima in the SAXS pattern can be attributed to the formation of shish-kebab structure in these positions.[12–25] In the case of 300 and 400 μm, the equatorial scattering maxima is very weak while the meridional maximum disappear absolutely, indicating the development of lamellae with low level of orientation. With a further increase in distance from 500 to

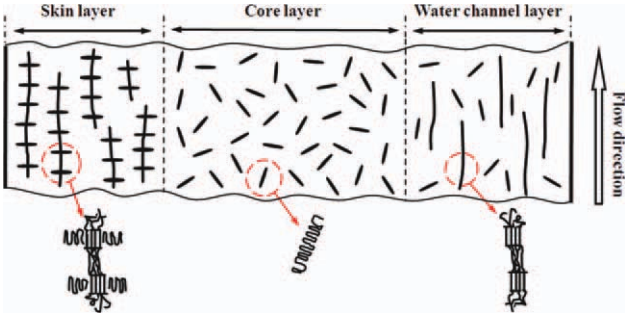

Figure 3 Schematic representing the distribution of crystalline morphology for the WAIM part across the residual thickness. [Color figure can be viewed in the online issue, which is available at wileyonlinelibrary.com.]

1400 μm, the 2D SAXS patterns show a clear circle-like scattering ring, which is an indicative of the absence of any detectable oriented structure. In the range from 1500 to 1800 μm, streak-shaped pattern (i.e., the meridional streak) and scattering ring are appeared again. However, these scattering rings' intensity is very weak, and it is even dimly visible at 1800 μm. This suggests the simultaneous development of bundles of parallel chains parallel to FD (i.e., shish) and the randomly aligned lamellae.

On the whole, one can easily find that the WAIM part is of multilayered structure, that is, the skin layer (from skin surface to 200 μm), core layer (from 300 to 1400 μm), and water channel layer (from 1500 μm to water channel surface). In view of this, the distribution of crystalline morphology for the WAIM part across the residual thickness can be illustrated in Figure 3. Clearly, this is consistent with the results reported in the literatures.[6–8] Though WAIM and gas-assisted injection molding (GAIM) have the similar processing procedure and the parts molded by the aforementioned polymer processing methods exhibit the identical macroscopical structure, the hierarchical structure of WAIM part is different from that of GAIM parts.[10,11] This should be ascribed to the different fluid mediums (i.e., water and gas) used in the two different polymer processing methods.

To determine the lamellar orientation distribution, the lamellar orientation parameter was calculated using the Hermans' orientation parameter, which is defined as follows[26]:

$$\langle P_2(\cos\phi)\rangle = \frac{(3\langle\cos^2\phi\rangle - 1)}{2} \quad (1)$$

where $\langle\cos^2\phi\rangle$ is an orientation factor defined as

$$\langle\cos^2\phi\rangle = \frac{\int_0^{\pi/2} I(\phi)\cos^2\phi\sin\phi d\phi}{\int_0^{\pi/2} I(\phi)\sin\phi d\phi} \quad (2)$$

where $I(\phi)$ is the scattering intensity at ϕ. The lamellar orientation parameters are calculated by eqs. (1) and (2) at different distances from the scattering intensity distribution along the azimuthal angle between 0° and 360°. Figure 4 is the azimuthal scans at different distances from the skin surface of WAIM part, by which the lamellar orientation parameters were calculated, and they are listed in Table I.

As shown in Table I, from 0 to 400 μm, the lamellar orientation parameter decreases sharply from 0.49 to 0.07. This is mainly due to the shear stress gradient along the thickness, which is brought by melt filling. In the region from 500 to 1400 μm, all the lamellar orientation parameter is 0, that is, the lamellae are randomly distributed. It is ascribed to the HDPE molecular relaxation and the relatively low cooling rate. Interestingly, from 1500 to 1800 μm, the lamellar orientation parameter increases slightly owing to the shear stress gradient brought by water penetration. But compared with the lamellar orientation parameter in skin layer, the lamellar orientation parameter in water channel layer is very small. This should be attributed to the relatively low temperature and shear stress brought by injected water.

The long period for the WAIM part

To obtain more insight into the superstructure of HDPE molded by WAIM, the typical one-dimensional (1D) SAXS curves at different distances from

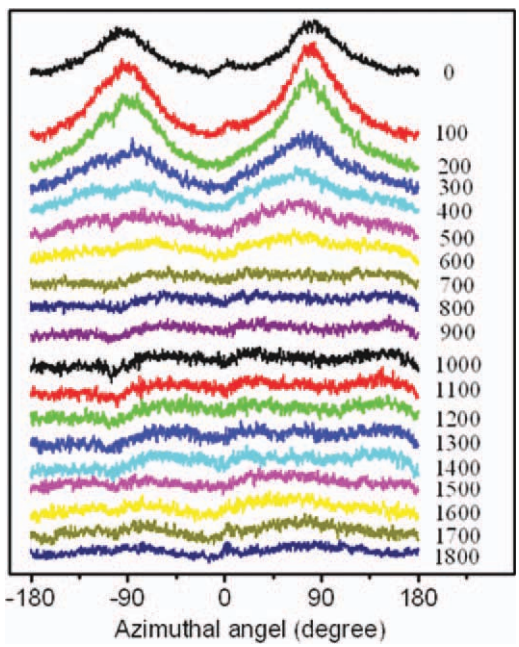

Figure 4 The corresponding azimuthal scans from Figure 2. The number (in μm) represents the distance away from the sample skin surface. [Color figure can be viewed in the online issue, which is available at wileyonlinelibrary.com.]

TABLE I
The Lamellar Orientation Parameters at Different Distances from the Skin Surface of WAIM Part

Distance (μm)	0	100	200	300	400	500–1400	1500	1600	1700	1800
Orientation parameter	0.49	0.44	0.33	0.18	0.07	0	0.03	0.08	0.14	0.16

the skin surface are shown in Figure 5. One can observe a typical scattering peak for HDPE existing in all 1D SAXS curves. The long period is related with the position of the scattering peak, which can be calculated from the peak position using the Bragg's law:

$$L = \frac{2\pi}{q} \tag{3}$$

with

$$q = \frac{4\pi \sin\theta}{\lambda} \tag{4}$$

where λ is the wavelength of the X-ray beam, θ is the scattering angle, and q is the scattering vector. The calculated long period is shown in Table II. Generally, long period in the positions from 0 μm to 800–1000 μm tends to elevate first and then that in the region from 1100 to 1800 μm, it decreases with the increase of the distance. That is, long period in the core of the WAIM part is the largest. Furthermore, it can be found that the value of long period in the water channel layer is very close to that in the skin layer.

DISCUSSION

As shown in Figure 1(a), WAIM and CIM have a same processing stage: melt filling. Therefore, to better understand the hierarchical structure of WAIM part, CIM part was also characterized at the selected positions from skin surface to the core by 2D SAXS. The corresponding results were shown in Figure 6 and Table III. In Figure 6(a), two distinct maxima along equatorial and meridional direction are observed in the positions from 0 to 200 μm, which indicates the existence of shish-kebab structure herein. At 300 μm, the equatorial scattering patterns are weak arcs and the meridional maximum also disappears completely, suggesting the formation of lamellae with low level of orientation. With a further increase in the distance from 400 to 4800 μm, the 2D SAXS patterns show a strong circle-like scattering ring, which indicates that isotropic morphology are dominant. The 2D SAXS patterns show that the CIM part exhibits a distinct skin-core structure, that is, the skin layer and the core region. Figure 6(b) is the azimuthal scans at different distances from the skin surface, by which the lamellar orientation parameters are calculated and listed in Table III. Clearly, the lamellar orientation parameter from 0 to 400 μm is declined from 0.45 to 0.03. In other positions, the lamellar orientation parameter is 0.

During the melt filling for both WAIM and CIM process, the shear stress reaches a maximum at the mold wall and a minimum in the core of the mold cavity. Furthermore, once the melt contacts with the cold mold wall, it is reasonable that the stretched and oriented molecules are prone to be frozen in the skin layer.[6,10–12] The larger shear rate causes a higher orientation of molecular chains. Simultaneously, a faster cooling rate slows down the relaxation and even freezes the orientation by the kick-in of crystallization.[10,11] Hence, the similar oriented structures formed in the skin layer of the WAIM and CIM parts should be ascribed to the identical melt filling. In this study, because of the larger diameter of the mold cavity (ca., 10 mm) and low heat conductivity of polymer, the heat of CIM part in the core transfers to the skin slowly and the cooling rate is small. It is well known that the orientation is a result of the competition between flow induced orientation and its subsequent relaxation. Based on these, it can be

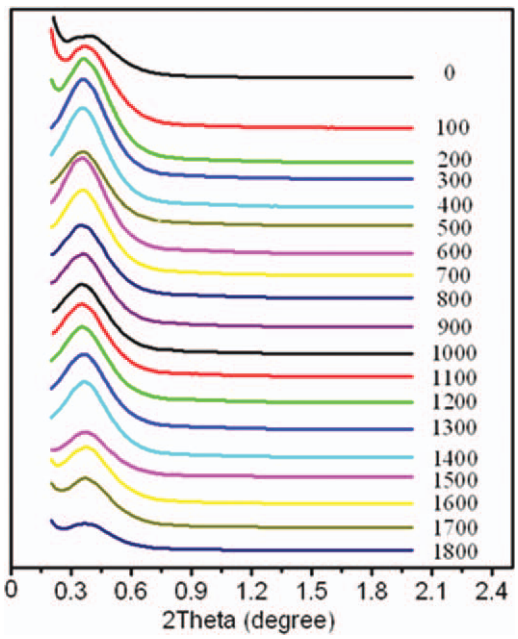

Figure 5 The 1D SAXS curves from Figure 2. The number (in μm) represents the distance away from the sample skin surface. [Color figure can be viewed in the online issue, which is available at wileyonlinelibrary.com.]

TABLE II
The Value of Long Period at Different Distances from the Skin Surface of WAIM Part

Distance (μm)	0	100	200	300	400	500	600	700	800	900	1000	1100	1200	1300	1400	1500	1600	1700	1800
Long period (nm)	22.2	23.4	23.4	24.7	24.7	24.7	24.7	24.7	26.1	26.1	26.1	24.7	24.7	24.7	24.7	23.4	23.4	23.4	23.4

envisaged that the oriented structures induced by the melt filling during the CIM process have longer time to relax compared with that in the WAIM process, which can be confirmed by the lamellar orientation parameters listed in Tables I and III.

In the case of WAIM process, following the melt filling, high-pressure water is injected into the core of the hot polymer melt. Once the high-pressure water enters the cavity, it shears and deforms the melt adjacent to the water channel surface. Meanwhile, it begins to cool the hot polymer melt therein. At the end of water penetration, most of the polymer melt in the core region is hollowed out by the injected water and the residual wall (ca., 1.8 mm) is formed. In the water packing and cooling stage, further thermal exchange will take place between the injected water and mold wall. In addition, owing to the high cooling capacity of the injected water, it is logical that the temperature of the residual wall will be decreased rapidly, and thus aligned kebabs were hardly induced by shish in the water channel layer. On the other hand, the water injection pressure (15 MPa) during the water penetration stage is lower than the melt injection pressure (75 MPa) in the melt filling stage. As a result, the lamellar orientation parameter in the water channel layer is smaller than that at skin layer. In the core layer of WAIM part, the low cooling rate and small shear stress allow the stretched chains to relax and consequently form spherulites with random lamellar orientation.

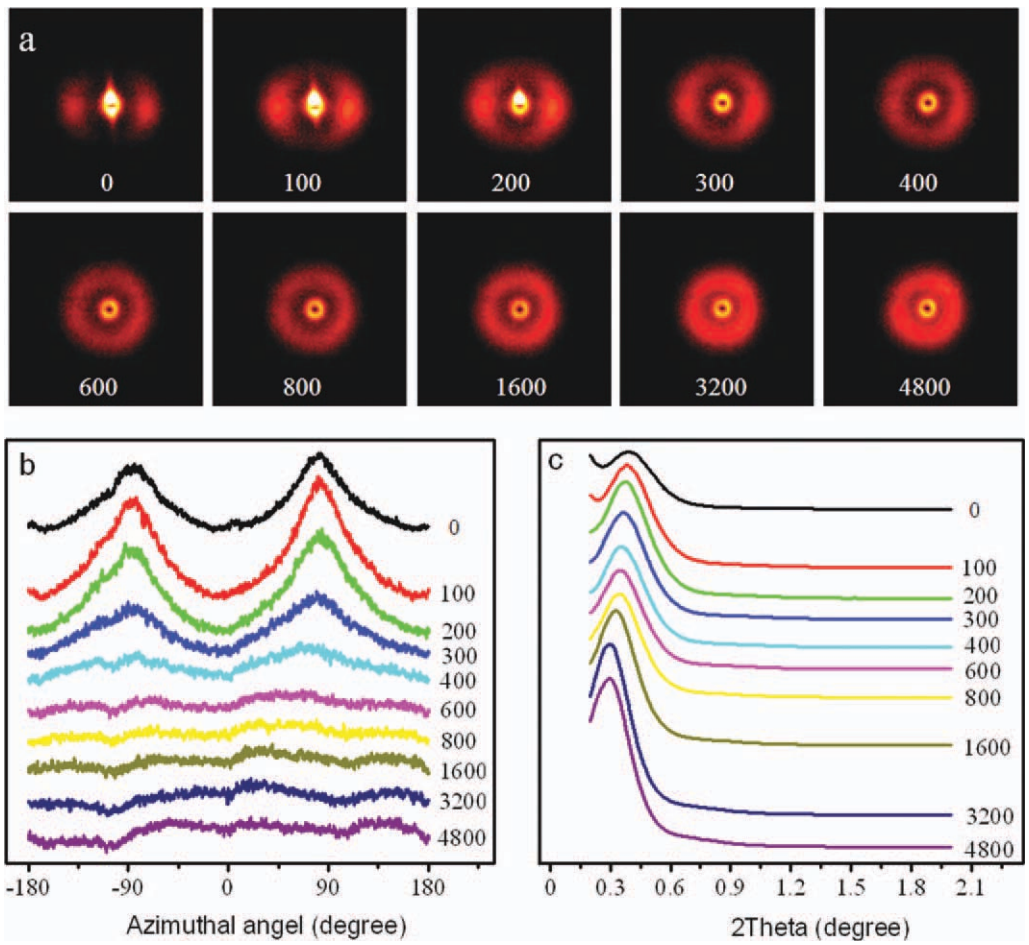

Figure 6 (a) 2D SAXS image patterns at the selected positions from the skin surface to the core of CIM part, (b) the corresponding azimuthal scans, and (c) the 1D SAXS curves. The number (in μm) represents the distance away from the sample skin surface. The flow direction is horizontal. [Color figure can be viewed in the online issue, which is available at wileyonlinelibrary.com.]

TABLE III
The Lamellar Orientation Parameters and the Values of Long Period of the CIM Part

Distance (μm)	0	100	200	300	400	600	800	1600	3200	4800
Orientation parameter	0.45	0.42	0.31	0.17	0.03	0	0	0	0	0
Long period (nm)	22.2	23.4	23.4	24.7	24.7	24.7	26.1	27.8	29.6	29.6

The typical 1D SAXS curves of CIM part at different distance are shown in Figure 6(c) and the values of long period are listed in Table III. It can be found that the long period of CIM part tends to increase monotonously with the increase of the distance from skin surface. According to the literature,[27] the shear field leads to a decrease of the long period. One can firmly deduce that shear field brought by the melt filling and water penetration are mainly responsible for the decrease of the long period in skin layer of both CIM and WAIM parts and that in water channel layer of WAIM part. In addition, it is well known that thinner crystal thickness is produced at lower crystallization temperature.[28] As mentioned above, due to the water penetration, cooling rate in WAIM part is more rapid than that of CIM one. Therefore, the long period of WAIM part is somewhat smaller than that of CIM part.

CONCLUSIONS

In this article, the hierarchical structure of HDPE parts molded by WAIM and CIM has been investigated by 2D SAXS. A distinct skin-core-water channel structure was observed across the residual thickness of WAIM part, while the CIM part shows a skin-core structure. In the skin layer, a similar oriented structure (shish-kebab) appears for both parts due to the identical shear stress brought by melt filling. Because the oriented structures of the CIM part induced by the melt filling have longer time to relax compared with that of WAIM part, the lamellar orientation parameter of WAIM part is larger than that of CIM part. Due to the low cooling rate and feeble shear strain, the random lamellae are dominant at the core layers of both parts. Furthermore, the shish structure companying the lamellae with low level of orientation emerges in the water channel layer of WAIM part. The shish structure is attributed to the shear stress brought by water penetration, while the low level of lamellae orientation is attributed to the high cooling capacity of the injected water. Therefore, the lamellar orientation parameter in the water channel layer is smaller than that of the skin layer. In addition, the long period of WAIM part first increases and then decreases with the elevating distance from the skin surface, while that of CIM part tends to increase monotonously. In a word, one can conclude that the rapid cooling rate and shear brought by the injected water have significant influence on the structural evolution for WAIM part.

The authors acknowledge the instructive advice for 2D SAXS measurement from Dr. Shao.

References

1. Liu, S. J.; Wu, Y. C. Polym Test 2007, 26, 232.
2. Liu, S. J.; Su, P. C. Polym Test 2009, 28, 66.
3. Liu, S. J.; Lin, M. J.; Wu, Y. C. Compos Sci Technol 2007, 67, 1415.
4. Liu, S. J.; Chen, Y. S. Compos Part A 2004, 35, 171.
5. Lin, K. Y.; Liu, S. J. Macromol Mater Eng 2010, 3, 342.
6. Liu, S. J.; Lin, W. R.; Lin, K. Y. Polym Adv Technol 2010, DOI: 10.1002/pat.1721.
7. Huang, H. X.; Deng, Z. W. J Appl Polym Sci 2008, 108, 228.
8. Huang, H. X.; Zhou, R. H. Polym Test 2010, 29, 235.
9. Fellahi, S.; Favis, B. D.; Fisa, B. Polymer 1996, 37, 2615.
10. Zheng, G. Q.; Huang, L.; Yang, W.; Yang, B.; Yang, M. B.; Li, Q.; Shen, C. Y. Polymer 2007, 48, 5486.
11. Zheng, G. Q.; Yang, W.; Yin, B.; Yang, M. B.; Liu, C. T.; Shen, C. Y. J Appl Polym Sci 2006, 102, 3069.
12. Wang, Y.; Gao, Y.;Shi J. J Appl Polym Sci 2008, 107, 309.
13. Chen, Y. H.; Mao, Y. M.; Li, Z. M.; Hsiao, B. S. Macromolecules 2009, 42, 4343.
14. Prasada, A.; Shroff, R.; Raneb, S.; Beaucage, G. Polymer 2001, 42, 3103.
15. Zhu, P. W.; Edward, G. Macromolecules 2004, 37, 2658.
16. Zhu, P. W.; Tung, J.; Edward, G. Polymer 2005, 46, 10960.
17. Zhu, P. W.; Edward, G.; Nichols, L. J Phys D Appl Phys 2009, 42, 1.
18. Caponetti, E.; Martino, D. C.; Cimmino, S.; Floriano, M. A.; Martuscelli, E.; Silvestre, C.; Triolo, R. J Mol Struct 1996, 383, 75.
19. Zhong, G. J.; Li, Z. M.; Li, L. B.; Mendes, E. Polymer 2007, 48, 1729.
20. Zhong, G. J.; Li, L. B.; Mendes, E.; Byeloy, D.; Fu, Q.; Li, Z. M. Macromolecules 2006, 39, 6771.
21. Na, B.; Zhang, Q.; Wang, K.; Li, L. B.; Fu, Q. Polymer 2005, 46, 819.
22. Wang, Y.; Na, B.; Fu, Q.; Men, Y. F. Polymer 2004, 45, 207.
23. Somani, R. H.; Hsiao, B. S.; Nogales, A.; Srinivas, S.; Tsou, A. H.; Sics, I.; Balta-Callejab, F. J.; Ezquerra, T. A. Macromolecules 2000, 33, 9385.
24. Somani, R. H.; Yang, L.; Hsiao, B. S.; Agarwal, P. K; Fruitwala, H. A.; Tsou, A. H. Macromolecules 2002, 35, 9096.
25. Agarwal, P. K.; Somani, R. H.; Weng, W. Q.; Mehta, A.; Yang, L.; Ran, S. F.; Liu, L. Z.; Hsiao, B. S. Macromolecules 2003, 36, 5226.
26. Picken, S. J.; Aerts, J.; Visser, R.; Northolt, M. G. Macromolecules 1990, 23, 3849.
27. Li, L. B.; De Jeu, W. H. Macromolecules 2004, 37, 5646.
28. Wunderlich, B. Macromol Phys 1976, 12, k11.